SPECIAL ISSUE REVIEWS–A PEER REVIEWED FORUM

Fluid Dynamics of Nodal Flow and Left–Right Patterning in Development

Julyan H.E. Cartwright,[1]* Nicolas Piro,[2] Oreste Piro,[3] and Idan Tuval[4]*

The manner in which the nodal flow determines the breaking of left–right symmetry during development is a beautiful example of the application of fluid dynamics to developmental biology. Detailed understanding of this crucial developmental process has greatly advanced by the transfer of ideas between these two disciplines. In this article, we review our and others' work on applying fluid dynamics and dynamical systems to the problem of left–right symmetry breaking in vertebrates. ***Developmental Dynamics 237: 3477–3490, 2008.*** **© 2008 Wiley-Liss, Inc.**

Key words: fluid dynamics; nodal flow; left–right patterning

Accepted 31 May 2008

INTRODUCTION

Understanding the process of determination of the left–right asymmetry in developmental biology is an inescapably interdisciplinary task, involving, as it does, fields ranging from molecular biology to fluid dynamics. Particularly interesting and surprising is the now well-accepted fundamental role that fluid dynamical phenomena play at the origin of the chiral differentiation process in at least some vertebrates. In a series of beautiful experiments published in 2002, Nonaka et al. (2002) convincingly showed that correct lateralization in mice is strongly correlated with the direction of the fluid flow induced within the node by a relatively small number of rotating 9+0 monocilia attached to the floor of this chamber. In normally developing embryos, this flow proceeds in a well-defined right–left direction, but if it is exogenously forced to reverse, the embryo develops *situs inversus*.

Rather than unravelling the mystery around the de novo generation of left–right asymmetry, these findings deepened the perplexity surrounding the phenomena by adding a physical asymmetry to the myriad of already reported asymmetric gene expressions. Several new unresolved questions emerged at that time: How does the clockwise motion of tens of monocilia drive a leftward flow in the node? And, if the observed flow is leftward, how is the fluid recirculating within the node, as it must, because the node is a closed structure? Finally, how does the nodal flow lead to left–right symmetry breaking in the embryo? These questions are within the realm of fluid physics.

The enigma of how a left–right-symmetric geometrical configuration of cilia could produce an asymmetric flow was resolved by us at the end of the same year using simple abstract symmetry arguments and fundamental hydrodynamics. Because at the lateralization stage, the embryo has already defined the dorsal–ventral and anterior–posterior asymmetry axes, the only chirally symmetric way to produce a chirally asymmetric flow is to use the tridimensional and pseudovectorial character of rotations. This led us to conclude that the clockwise-

[1]Instituto Andaluz de Ciencias de la Tierra, CSIC–Universidad de Granada, Campus Fuentenueva, Granada, Spain
[2]ICFO-Institut de Ciencies Fotoniques, Mediterranean Technology Park, Castelldefels (Barcelona), Spain
[3]Dept de Física e Instituto de Física Interdisciplinar, y Sistemas Complejos IFISC (CSIC-UIB), Universitat de les Illes Balears, Palma de Mallorca, Spain
[4]Department of Applied Mathematics and Theoretical Physics, University of Cambridge, Cambridge, United Kingdom
Grant sponsor: Spanish Ministerio de Ciencia y Tecnología; Grant number: FIS2005-07083-C02-02; Grant sponsor: CSIC agency HIELOCRIS;
Grant number: 200530F0052; Grant sponsor: the Human Frontier Science Program.
***Correspondence to: Idan Tuval, Department of Applied Mathematics and Theoretical Physics, University of Cambridge, Cambridge CB3 0WA, UK. E-mail: i.tuval@damtp.cam.ac.uk or Julyan H.E. Cartwright, Instituto Andaluz de Ciencias de la Tierra, CSIC–Universidad de Granada, Campus Fuentenueva, Granada E-18071, Spain. E-mail: julyan@lec.csic.es**

DOI 10.1002/dvdy.21672
Published online 4 September 2008 in Wiley InterScience (www.interscience.wiley.com).

Developmental Dynamics

rotating cilia should be tilted toward the posterior end of the node. By means of a very simple minimal model of the system where the cilia were idealized as elementary point rotators (rotlets) we were able first to rule out an existing alternative hypothesis that the origin of the flow was related to the shape of the node, and then to estimate the tilt angle of the cilia from the measured velocity of the flow and the observed rotation frequency of the cilia. It is important to remark that this prediction predated the actual measurement of the detailed structure of the cilia and the experimental demonstration that this tilt indeed existed in real embryos. Even more notable was the quantitative confirmation of the tilt angle predicted a priori from the theory (Cartwright et al., 2004).

The history of this discovery is instructive with respect to the possible ways that general physical thinking may best contribute to interdisciplinary endeavors such as the development of this subject. There is a strongly implanted tendency in applying physics to biology to build models a posteriori to describe mathematically the existing data. This modeling philosophy reduces the role of mathematical physics to a sort of painting tool to produce sophisticated pictures of a given phenomenon. But while a picture may be extremely beautiful, realistic, and detailed, it is just a picture, generally void of any predictive power to explore unknown aspects of the phenomenon. We maintain that a more useful approach is essentially the opposite. In the same artistic metaphor we advocate a more modernist and abstract attitude, discarding unnecessary details that distract the attention from the deep and fundamental aspects of a problem so that we can concentrate in well-defined creative proposals to look at a given problem in a new and different way.

In what follows we review the fluid dynamical models of the nodal flow proposed in the literature. We explain their limitations and the predictions drawn from them, and we compare them with the latest available experimental data.

NODAL FLOW: A MINIMAL MODEL

The node is a liquid filled chamber present in the early stages of growth of vertebrate embryos. At the time of gastrulation, the mouse embryo, the most studied case, is essentially a flat, two-layered sheet, with a groove in the middle called the primitive streak, and a dimple at the anterior end named Henson's node. Roughly pear shaped when viewed from above—that is, from the ventral side—some 50 μm across, and 10–20 μm deep, the node is covered by Reichert's membrane, and filled with extraembryonic liquid; see Figure 1. Arrayed over its base are a few tens of monocilia some 2–3 μm in length. These are cylindrical in cross section, and are seen to rotate clockwise as viewed from above, at frequency f circa 10 Hz (Nonaka et al., 1998, 2002), and to move fluid from right to left at approximately 20–50 $\mu m\ s^{-1}$ in what is now known as the nodal flow.

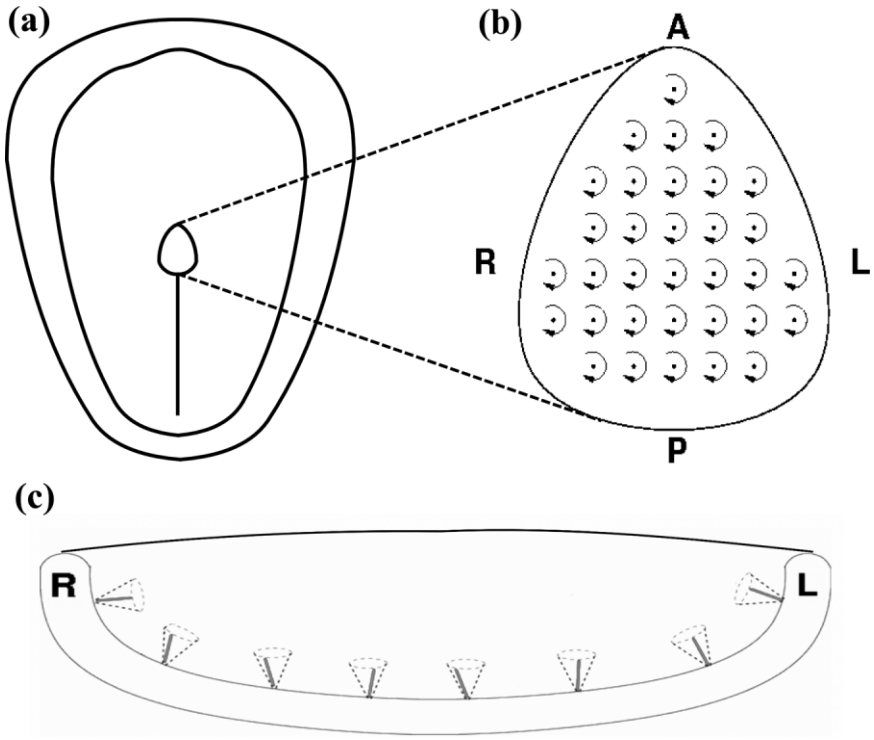

Fig. 1. **a:** Position of the node and the primitive streak in the mouse embryo. **b,c:** Ventral (c) and posterior (b) sketch views of the node of the mouse embryo, and its rotating monocilia. Note that, following the convention in this field, in this and all subsequent vertical slices of the node shown the node is seen from the ventral side, and thus the left side of the embryo is on the viewer's right.

Different approaches have been put forward to investigate transport in the nodal flow. An exhaustive modeling effort should contain elements at various levels, linking the bio-molecular machinery to the ciliary dynamics; the ciliary dynamics to the nodal hydrodynamics; the fluid flow to the signaling transport; and finally the feedback from the macroscopic transport to the bio-molecular and genetic signaling cascade. All these processes are essential for the correct development of vertebrate left–right asymmetry and need to be incorporated in any model aiming to explain it in detail. However, before such a model can be built, modeling of the separate elements will help us to explore the essentials of the process by providing partial answers to the unknown mechanisms. In what follows we focus on the macroscopic level, exploring both the nodal hydrodynamics and the signaling transport by the nodal flow.

As we are interested in understanding the fluid flow generated by an array of rotating monocilia in the node, our starting point has to be the Navier–Stokes and continuity equations which describe the motion of a viscous incompressible fluid. These equations are:

$$\frac{\partial \mathbf{u}}{\partial t} + (\mathbf{u}\cdot\nabla)\mathbf{u} = -\frac{1}{\rho}\nabla p + \upsilon\nabla^2\mathbf{u} + \frac{1}{\rho}\mathbf{f}_{\text{ext}} \tag{1}$$

$$\nabla \cdot \mathbf{u} = 0,$$

where ρ is the fluid density, p the pressure, $\mathbf{u}$ the velocity, υ the viscosity, and $\mathbf{f_{ext}}$ the external force.

For a steady (time-independent) flow the first partial derivative vanishes. The character of a steady viscous flow depends strongly on the relative magnitudes of the terms $(\mathbf{u}\cdot\nabla)\mathbf{u}$ and $\upsilon\,\nabla^2\mathbf{u}$ in the equation of motion. To compare them, we must put the equation into a dimensionless form. To do this, we redefine the variables $\mathbf{u}$, t, p, and $\mathbf{f_{ext}}$, dividing them by a characteristic length scale L of the flow, a characteristic velocity U, a characteristic pressure P, and a characteristic force F. The Navier–Stokes equation then reads

$$(\mathbf{u}\cdot\nabla)\mathbf{u} = -\nabla p + \frac{1}{\mathrm{Re}}\nabla^2\mathbf{u} + \mathbf{f}_{\mathrm{ext}} \quad (2)$$

where Re, the Reynolds number, measures the relative importance of inertial to viscous forces in the flow:

$$\textit{inertial force} \sim |\mathbf{u}\cdot\nabla\mathbf{u}| \approx \frac{U^2}{L},$$

$$\textit{viscous force} \sim |\upsilon\nabla^2\mathbf{u}| \approx \frac{\upsilon U}{L^2}, \quad (3)$$

$$\mathrm{Re} = \frac{UL}{\upsilon} \approx \frac{\textit{inertial force}}{\textit{viscous force}}.$$

The flow velocity produced by the monocilia has been measured with passive tracers to be some 20–50 μm s^{-1} in wild-type embryos (Okada et al., 1999). Taking ν, the kinematic viscosity of the extraembryonic fluid as that of a dilute aqueous solution of proteins, this suggests that the Reynolds number of the node is of order 10^{-3}. We can obtain another Reynolds number from the cilium rotation velocity: $\mathrm{Re_c}=\omega l^2/\nu$, where ω is the angular velocity $2\pi f$ and l is the length of a cilium, from which $\mathrm{Re_c}\sim 5\times10^{-4}$. The two estimates are close, and, whether we take $\mathrm{Re_n}$ or $\mathrm{Re_c}$ as the more representative, the Reynolds number of the flow is certainly very low. This means that viscosity dominates inertia; if the monocilia were to stop, the flow would instantly cease. Under this condition, known as creeping flow, the Navier–Stokes equations that describe the movement of fluid may be linearized to the Stokes equations, which are amenable to analytical solution.

$$\nabla p = \frac{1}{\mathrm{Re}}\nabla^2\mathbf{u} + \mathbf{f}_{\mathrm{ext}} \quad (4)$$

An important feature is that the Stokes equation is a linear equation in $\mathbf{u}$. This means that if $\mathbf{u}_1$ and $\mathbf{u}_2$ are two velocity fields that satisfy the equation, a superposition of them is also a solution. So one can try to find simple solutions of the Stokes equation, and then using its linearity property, one can describe a more complex situation as a superposition of the simple solutions.

With this idea, one can solve the Stokes equation for a point force $\mathbf{f}_{ext}(\mathbf{x}) = \delta(\mathbf{x})\cdot\vec{f}$ using Fourier transforms and Green's theorem (Batchelor, 1970; Brennen and Winet, 1977; Currie, 1993). Then, any situation where there is some phenomenon which could be modeled as a collection of point-force may be solved directly as an appropriate combination of these point-force solutions. The point-force solution is named a Stokeslet (Hancock, 1953; Currie, 1993). Some related flows fields may be constructed from the original point-force flow field. For example, any gradient of the original solution is a solution to the problem associated with the gradient of the original force. These gradients are dipoles, quadrupoles, and so on. Moreover, the solution of the Stokes equation with a point-torque force term can be constructed from the Stokeslet model. This solution named a rotlet represents the flow produced by a rotating sphere in the limit that its radius vanishes while keeping the angular velocity constant (Chwang and Wu, 1975; Currie, 1993) and is given by:

$$\mathbf{u} = \frac{T\times\mathbf{x}}{8\pi r^3}$$

where $\mathbf{T}$ is the applied torque, $\mathbf{x} = (x,y,z)$ the coordinate in three dimensional space, and $r = \sqrt{x^2+y^2+z^2}$ the distance from the origin.

As the monocilia lining the floor of the node rotate, each produces a vortex about itself in the flow. This vortical flow can be modeled at a first order by a rotlet as is shown in Figure 2a. Then, an array of vortices is simply a combination of rotlet solutions with the same topology as the array of rotating monocilia in the node. This corresponds to the minimal rotlet model introduced in Cartwright et al. (2004). Before investigating more complex models that supplement specific details, let us explore the essence of the system by means of this minimal model.

We integrate the equation of motion of a fluid element following the flow generated by a rotlet $\dot{\mathbf{x}} = \mathbf{u}$, with $\mathbf{u}$ given by Eq. 4. We first take the torque perpendicular to the node floor (assumed to be the xy plane), thus modeling a vertical cilium located at the origin and rotating with $\mathbf{T} = (0,0,T)$. We plot the resulting trajectories for different initial conditions in Figure 2a. We then model an array of rotating monocilia by an array of N rotlets distributed on the xy plane. The resulting velocity field is simply the sum of the N different $\mathbf{u}_i$ generated by the rotlets, from the linear property of the Stokes equation discussed above.

$$\mathbf{u}_{\mathrm{total}} = \sum_{i=1}^{N}\mathbf{u}_i$$

We integrate once more the equation of motion for a fluid element: in Figure 2b, the cilia are rotating with vertical axes as in Figure 2a, but now distributed in a rectangular array. One hundred initial conditions are used and the torque has been taken to be equal for each rotlet. If the monocilia rotate about vertical axes, they create a set of vortices, one per cilium, but not a directional flow in the fluid above. Instead, as depicted in Figure 2b, there is a flow consisting of a cellular network of vortices, in which a general circulation only occurs at the edges of the network; elsewhere, movement is vertical. This does not correspond with the experimental observations of a general leftward flow above the cilia. Nonaka et al. (1998, 2002) suggested that the key to producing such a flow is in the shape of the node; it is elongated, or pear shaped (Fig. 1), and so the array will be not a rectangle, but a triangle of vortices. However, merely changing this aspect of the geometry does not qualitatively change the flow field; it is still vortical within the triangular array, with a general circulation only at the edges. A further possibility would be cilia shaped like oars, which, if feathered during part of the rota-

tion, could produce a directional flow; but all observations show cylindrical cilia. To envisage how a general circulation within the node may be produced by cylindrical cilia, a useful analogy is to a kitchen blender; if this is held vertically in the fluid it is mixing, so that the blades rotate about a vertical axis, the surface flow is a vortex around the stem of the blender. But if the blender is tilted, the surface shows a general flow in the direction in which the blades are turning when they are closest to the surface. In the node, then, we should consider the possibility that the cilia are all inclined, so that they sweep out circles at an angle to the horizontal. If each one is tilted in the same direction, there will be a directional flow across the chamber above them, due to the fluid overhead being entrained in their direction of rotation; the greater the tilt, the stronger the directional flow above the vortices. It may be objected that this tilt suggests a prior symmetry-breaking event. This is so, but the symmetry broken is the already defined anterior–posterior axis, and not left–right; for to obtain the observed leftward flow, given that they rotate clockwise, the monocilia ought to be tilted toward the posterior.

Consider a single rotlet as in Figure 2a, but now inclined at an angle α to the vertical. For a general leftward flow as is seen in the node to emerge from a cellular network of such vortices, what angle of tilt α would be necessary? We can estimate this from the observed tip velocity $V_{tip}=2\pi af$ of a cilium and the flow velocity U of the nodal fluid. Close to the tips of the cilia, the flow velocity will match the tip velocity. The component of the tip velocity contributing to a directional flow is $V_{tip} \cdot \sin(\alpha)$, so we can estimate $\alpha=\arcsin(U/2\pi af)$. If we substitute the ranges of values for U, α and f mentioned earlier, we find the angle of tilt to be around 25° from the vertical. We model such an array of tilted rotlets in Figure 2c. A rectangular array is used again, but now, the rotlets are inclined at an angle α to the vertical toward the posterior direction y, in such a way that the respective torque is given by $\mathbf{T} = (0,-T \sin \alpha, T \cos \alpha)$. In each case, one trajectory is highlighted in a different color in the figures for better visualization purposes. We see that a directional flow above the rotlets arises exactly as predicted.

From the biological point of view, one can envisage two possibilities for inclined cilia: either the inclination is active, requiring the shaft to bend and straighten during one period of the circling movement, or it is passive, with the embedded base of the cilium inclined at an angle and no change in the magnitude of the bending of the shaft being necessary. This rotlet model covers both these cases, as the fluid dynamics is substantially the same, and with either passive or active inclination, the cilia must be oriented toward the posterior as they rotate.

In the hierarchy of possible models for the nodal flow, our aim has been to choose to use that one with the minimal complexity necessary to explain the observations. However, a pertinent question emerges. How good is our approximation? We have simplified the hydrodynamical problem in several ways:

We model the flow induced by a rotating cilium as a vortex, as if instead of the cylindrical paddle that is a cilium, there were an infinitesimal sphere rotating in its place. This is a good approximation to the induced flow, especially at the low Reynolds numbers present in the node, where there are no inertial effects. A further step would be to model each cilium in detail. Some attempts in that direction are based on distributions of fundamental singularities—Stokeslets and derived solutions—along the cilium or flagellum length and on slender-body approximations (Brokaw, 1972; Blake, 1972; Lighthill, 1976; Smith et al., 2007), although in these cases a prescribed form of the beat is imposed. Other work incorporates the coupling between the molecular motors driving ciliary dynamics and the viscous and elastic forces, both at the level of the whole cilium or flagellum (Gueron and Liron, 1992; Gueron et al., 1997) and at the level of the individual protein structures of the axoneme (Dillon et al., 2000; Brokaw, 2005). These phenomenological models for the coupling have been developed both for 9+2 and 9+0 cilia and have been complemented with a range of hydrodynamical approaches to give an accurate representation of ciliary dynamics.

Most of these models describe the time-dependent dynamics of a cilium, which allows for a more detailed representation of the nodal flow. This description is more relevant near the moving cilium surface where time averaged modeling will not be accurate. Nevertheless, the numerical simulations in those works support the hypothesis that nothing essential is left out in the simpler model we discussed above, although they raise several interesting questions. For instance, there is a fundamental puzzle regarding the details by which the rotational symmetry is broken and the clockwise rotation is generated. In this respect the work by Brokaw (2005) shows how the structural chirality of the axoneme can be transformed into an effective control of the circling direction if there is a unidirectional information transfer from doublet to doublet.

Another open question is the reason for the differing behavior observed during different stages of ciliary rotation (Okada et al., 2005). Flagella with a 9+2 structure are known to present a biphasic beat pattern that may be decomposed into an effective and a recovery stroke. Buceta et al. (2005) proposed a similar dynamics for the 9+0 nodal cilia invoking exogenously introduced stroke changes in different stages of the cycle. However, the theoretical investigation by Dillon and Fauci (2000) showed that many interesting features of the detailed dynamics of the cilia can emerge spontaneously. Hence, is this differential behavior the result of the particular structure of the cilium, as suggested by the Buceta et al. model, or is it the necessary consequence of the interaction of an elastic structure moving at low Reynolds number in a fluid near a wall? Such an important question should be addressed and resolved by means of specific predictions that could be checked experimentally, but this has not been done so far either theoretically or experimentally. In this regard, it is worth noting that if the nodal flow is the first left–right symmetry breaking event, 9+0 cilia could not be replaced by 9+2 cilia with a planar beat, because to produce a flow toward the left, these would have to be orientated along an already defined left–right axis. The 9+0 cilia on the other hand can produce leftward

flow using only their whirling in a given sense together with an orientation toward the posterior on the already defined anterior–posterior axis. This morphological difference is then fundamental to their role in initiating left–right symmetry breaking, which should be born in mind when postulating possible differential strokes in different parts of the cilium cycle.

It is also possible to conceive even simpler nodal flow models than those we have discussed: toy models, which are not solutions of the Navier–Stokes equations, but merely caricatures of them. We have fruitfully used such models in our work in other circumstances (Babiano et al., 2000; Cartwright et al., 2002). Such toy models cannot, however, be easily adapted to the present instance—they are generally two-dimensional models, and similar ideas in three dimensions that respect all the flow requirements are much harder to construct—and in any case are unsatisfactory when it is possible to use a model which does represent a solution of the fluid equations. For these reasons Stokeslet and rotlet models were developed (Hancock, 1953; Batchelor, 1970; Chwang and Wu, 1975; Currie, 1993); these ideas were originally developed with a biological application in mind: that of microbial swimming (Brennen and Winet, 1977). Lately, they have been used to model chaotic advection (Meleshko and Aref, 1996), and another application to biological problems is a model of the filter feeding mechanism in bivalve molluscs constructed with Stokeslets (Blake and Otto, 1998). As much of biological fluid dynamics is at the microscale—at low Reynolds numbers (Purcell, 1977)—we anticipate that this approach will prove to have many more fruitful applications in biology.

In the foregoing simulations with a minimal model, we have implicitly idealized the node enormously. Although the pertinent fluid-dynamical variable, the Reynolds number in the node, has been set to be the same in the simulations as in the real mouse node, so we can be confident that the fluid flow is likewise the same, we have neglected the important role the presence of boundaries plays in defining the specific features of the flow. This will be discussed in detail in the next section.

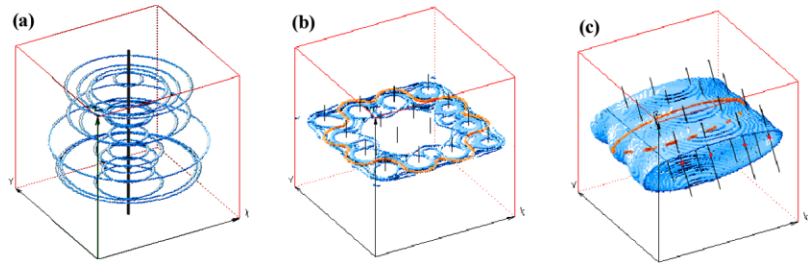

Fig. 2. **a:** Vortical flow structure produced by a single rotlet. **b:** Rectangular array of rotlets with axes vertical, showing cellular structure of vortices with a general circulation only occurring at the edges. **c:** Result of tilting the rotlet axes: array of tilted rotlets with tilt angle $\alpha = 24°$, showing directional flow above and below the array.

NODAL FLOW: DIRECT NUMERICAL SIMULATIONS

One thing the initial minimal model of nodal flow intentionally left aside was the complicated analysis of the nearby boundary effects on the flow induced by tilted cilia within the node. When concentrating on obtaining a good estimate of the tilt angle in terms of the observed strength of the main flow, it is necessary to focus on the sources of the flow and forget momentarily the complexity of the perturbations suggested by the boundaries. The price to pay for such a radical simplification is, of course, the appearance of undesired symmetries that would have been broken by the boundaries. In the present case, this obliges us to live in that model with an artificially strong return flow accompanying the observed one. It was, however, advanced that this flow would be strongly suppressed once the boundary conditions were properly taken into account (Cartwright et al., 2004).

Based on the generic behavior of Stokes flows in closed chambers, we suggested (Cartwright et al., 2004) a

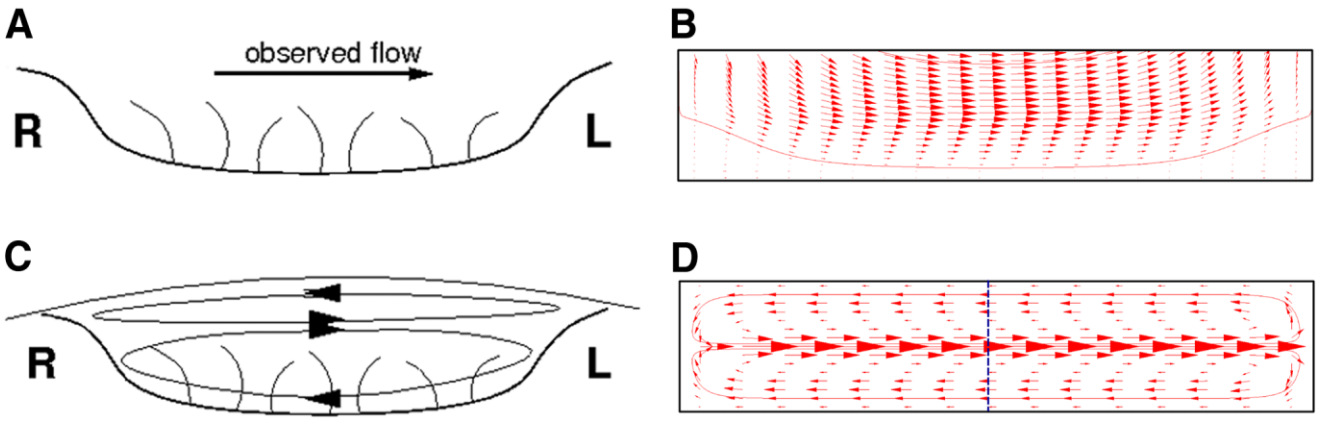

Fig. 3. **a,c:** Sketch of how fluid will recirculate within the node (a) in vitro and (c) in vivo. **b,d:** Vertical views corresponding to *y*-direction averages of the velocity field in the node from direct numerical simulations: in vitro (b) and in vivo (d). The dashed line in d represents the cross section depicted in Figure 4.

plausible geometry that takes into account in a qualitative manner the presence of boundaries. This geometry consists of a strong and well-defined right–left flow induced by the ciliary motion complemented by two much slower and chaotic return flow components required by mass conservation located near the floor and the ceiling of the node. It is worth emphasizing that while both return flows are a trivial necessity imposed by mass conservation, the bottom flow is also strongly conditioned by the presence of the cilia, which makes it much more irregular.

We later confirmed the proposed flow structure by performing full scale fluid dynamical simulations of the whole system, taking into account not only boundary conditions but also the finite size of the rotating cilia (Cartwright et al., 2007). In these simulations, we represented the node by a fluid-filled box of dimensions $50 \times 50 \times 10$ μm, either completely closed as in vivo, or open at the top and placed within a much larger fluid-filled volume to model the in vitro bead-tracking experiments, which take place in such an experimental setup. We solved the steady-state Navier–Stokes equations for the nodal fluid set into motion by cones that form the surfaces of revolution of the cilia (length 3 μm; half-angle 45°; rotation frequency 10 Hz) rotating clockwise viewed from above inclined at an angle $\alpha = 25°$ to the posterior. The ciliary Reynolds number in these simulations is of order 10^{-4}.

We present a broad view of the circulation in the in vivo and in vitro nodal flows from these simulations in Figure 3. In both the in vivo and the in vitro node there is a general leftward flow across the centre of the node that corresponds well to that observed in experiments. In the in vivo case, this fluid recirculates within the node following the walls, so the general scheme is of two vortices, one in each of the upper and the lower halves of the node; fluid flows to the left across the middle and returns to the right along the ceiling and floor of the node. The flow in the lower vortex is more complex than in the upper vortex owing to the presence of the cilia; while there is a general recirculation across the floor of the node, some pathlines representing fluid parcels become trapped in the vicinity of a cilium and may spend some time there before rejoining the general circulation. In contrast, in the in vitro case, the opening of the node with the removal of its covering membrane completely eliminates the upper recirculatory vortex within the node. Fluid is now free to enter and leave the node to flow around a much larger surrounding volume, so the upper recirculation occurs around the whole of the box containing the node. As the fluid volume is larger, velocities are lower, and the rightward return current occurs far beyond the limits of the node in a manner so diffuse as to be almost imperceptible compared with the leftward flow within the node. The strong leftward current above the cilia is, as before, the most prominent feature of the flow. The flow in the lower half of the node, below the leftward current, persists, but the general rightward component is diminished compared with recirculatory flow about individual cilia. Thus, while the main feature of the nodal flow, the central leftward current, is present in both in vivo and in vitro, there are significant differences in other aspects of the two flows. This should make one wary of using in vitro bead tracking experiments as the sole basis for understanding the in vivo flow; they ought to be interpreted together with a knowledge of the differences between the in vivo and in vitro flows.

Although the upper recirculatory vortex has been experimentally observed (Okada et al., 2005), the existence of the lower vortex has been doubted and both experimental (Nonaka et al., 2005) and theoretical (Smith et al., 2007, 2008) works have attempted to explain this disagreement by focusing on the role that cilia–node–floor interactions play in determining the fluid dynamics in the node. They have also correctly accounted for the unsteady nature of cilia dynamics. However, while the details of the above-mentioned interaction are certainly important for the appropriate modeling of this system, these models obscure the most basic reason behind the existence of a return flow. In the same way that the upper recirculatory vortex does not have to be triggered by a rightward "active" phase in the ciliary beating pattern, the existence of the lower vortex is not solely determined by the rightward motion of the cilia when passing near the node floor. In both cases, only two basic features are necessary: the symmetry of the sources of force density in the Stokes equation and the unavoidable observance of volume conservation by the fluid. If these two premises hold then, even in the absence of a rightward phase in the ciliary dynamics caused by no-slip boundary conditions, the proposed return flow pattern will emerge.

Therefore, to understand the actual fluid dynamics, a detailed study of the symmetries involved is essential. In particular, a two-vortex pattern is suggested by symmetry when the length of the cilia l is comparable to half the node depth d. It is this parameter—the ratio of cilia length to node depth—that is the most important for the determination of the correct flow structure given the symmetries already present in the other axes. We show here simulations describing the vortex structure as a function of l/d. In all cases, the correct boundary conditions, and therefore the cilia–node floor interaction, are taken into account. But, in contrast with previous studies (Buceta et al., 2005; Smith et al., 2007, 2008), these simulations account for the closed structure of the node, emphasizing the crucial role that this feature plays in determining the return flow. We show in Figure 4 that the two-vortex structure for an in vivo node is, independently of the cilia–node floor interaction details, a solution of the fluid dynamical problem. However, the strength of the lower vortex compared with the upper one is strongly dependent on l/d, varying from a symmetric biphasic structure for $l/d=0.5$ to the almost complete disappearance of the lower return flow for small l/d. In the murine node the cilia are of length approximately 3 μm, and in previous work we used a value of 10 μm for the node depth, under which conditions the lower return flow is appreciable. However, if one takes into account the curvature of Reichert's membrane in vivo a figure of some 20 μm may be more appropriate under physiological conditions, in which case we may estimate $l/d \sim 0.1–0.2$. Under these circumstances the combination of the weakness of this vortex and its complicated structure, owing to the presence of the

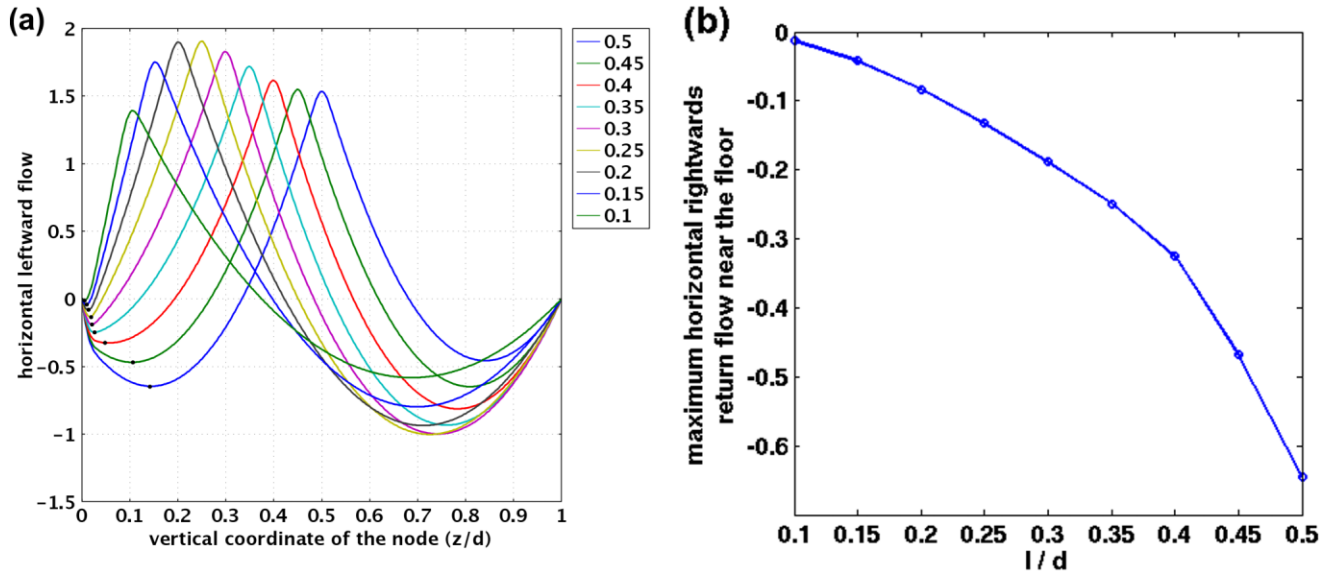

Fig. 4. Dependence of the lower recirculatory vortex on the ratio between cilia length and node depth l/d. **a:** Leftward velocity in a vertical cross section of the node showing the presence of two return flows for different values of l/d. The position of the maximum lower return flow is marked by dots. **b:** Strength of the lower recirculatory vortex as a function of l/d.

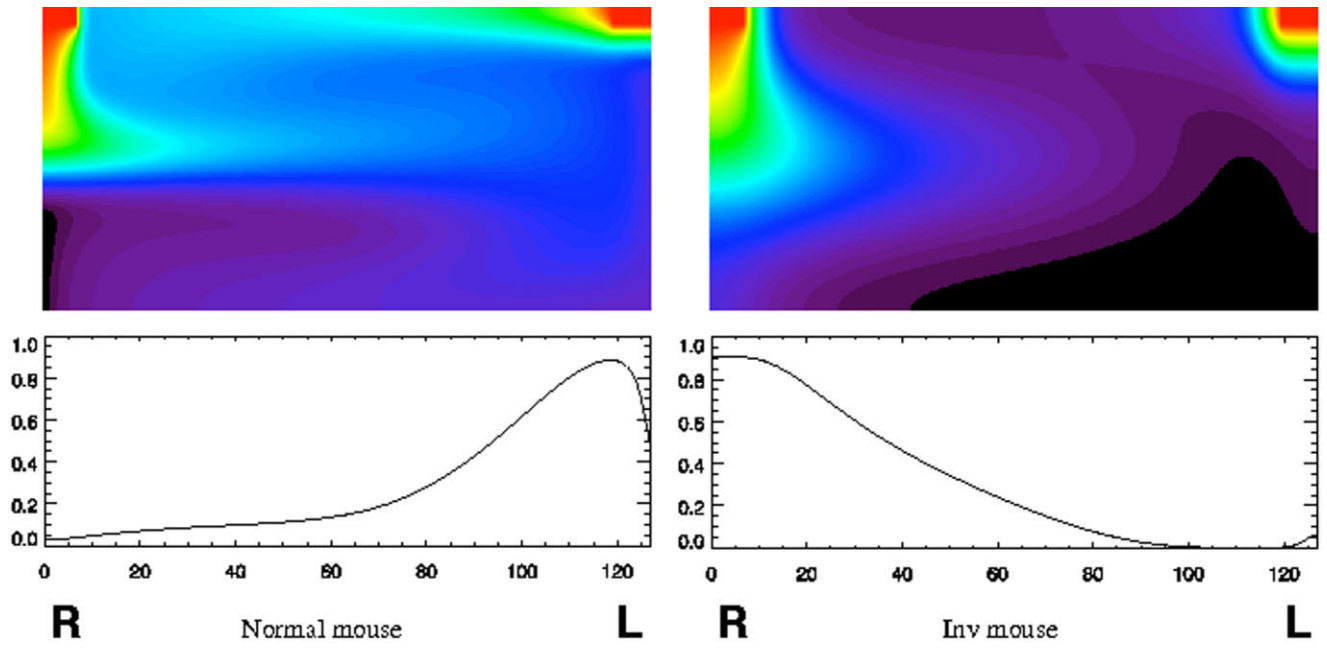

Fig. 5. **a,b:** Numerical simulations depicting the steady-state concentration of a morphogen with a finite lifetime within the node for wild-type (a) and *Inv* (b) mice. The color scale is as for a rainbow, with red the highest concentration, and violet the lowest. **c,d:** Graphs of the concentration of morphogen at the floor of the node in the above simulations with wild-type (c) and *Inv* (d) mice (arbitrary units).

cilia, would make it difficult to observe even under ideal in vivo conditions, not to mention under the conditions usual in vitro experiments. Hence the lower recirculatory flow will be observable only in shallower nodes.

Experimental verification of the precise global structure of the nodal flow is still incomplete. Despite the impressive advances produced by the powerful experimental techniques that have been recently developed to visualize directly both the nodal flow and the ciliary motion, some of these are deeply invasive in a functional sense. While a murine node in vivo is basically a closed chamber, in experiments conducted with mice Reichert's membrane is removed for visualization purposes; a maneuver that, as we discussed above, produces a radical modification of the flow from its in vivo conditions unless the chamber is carefully resealed. For the transpar-

ent embryos of zebrafish this operation is not necessary and the equivalent structure, Kupffer's vesicle, is observed noninvasively (Essner et al., 2005; Kramer-Zucker et al., 2005). Still, our incomplete knowledge of the detailed structure of the nodal flow is a fundamental obstacle to achieving an unambiguous understanding of the mechanism by which the macroscopic structure of the flow produces the differentiation across the symmetry axis. Nevertheless, it is worth noting that the existence or not of any return rightward flow seems not to be fundamental for the correct determination of embryo lateralization. This is experimentally true as in vitro embryos with Reichert's membrane removed, and consequently in the absence of the upper vortex within the node, display the same left–right asymmetry as in vivo embryos. This fact is also completely compatible with the proposed theoretical mechanisms for the generation of gene expression asymmetries by the nodal flow; these are not based on the existence of any particular recirculatory pattern, as we will show in the next section.

PASSING THE FLOW INFORMATION TO THE EMBRYO

How is the information on the symmetry broken by the nodal flow transmitted to the embryo? Two means have been proposed: chemosensing and mechanosensing. On one hand, it has been suggested that the nodal fluid may be carrying a morphogen, a signaling molecule—probably a protein—that is released into the flow, and whose concentration is detected by chemoreceptors within the node (Nonaka et al., 1998). On the other, more recent experimental work has shown that there appear to be two populations of monocilia in the node, and it has been speculated that the second population may be nonrotating mechanoreceptors (McGrath et al., 2003). Below, we first treat the original morphogen hypothesis, and discuss a model for morphogen transport and mixing in the node compatible with the observations and with the physics. We then discuss why mechanosensing is unlikely to be the mechanism operating in the node. Finally, in the following section, we examine a variant of the original morphogen idea motivated by more recent experimental evidence: the hypothesis that it is the transport of nodal vesicular parcels (NVPs), packets containing morphogens, that is responsible for the transmission of the flow asymmetry into an asymmetric signaling cascade.

The flow structure explored in the previous section gives support to a possible robust mechanism of gradient formation for the morphogen concentration. Namely, the combination of three processes: advection or the hydrodynamical transport of a given substance, molecular, or another type of, diffusion and a chemical deactivation reaction. Mathematically, this is expressed in terms of a so-called advection–reaction–diffusion (ARD) partial differential equation whose input should be the flow scheme including its characteristic intensity U and the relevant diffusion D_c and decomposition or deactivation rates κ. The source of morphogens can also be added into this equation explicitly or in the form of appropriate initial and boundary conditions.

$$\frac{\partial c}{\partial t} + u \cdot \nabla c = D_c \nabla^2 c - \kappa c$$

If the balance between these three elements is correct, a gradient in the morphogen concentration can build up in the appropriate direction to trigger the differentiation between the left and the right sides of the developing embryo. Moreover, alterations of this balance originated in the debilitation of the right–left flow outside of a given range can be shown to produce the opposite gradient, which may explain the origin of the large proportions of situs inversus in some genetically originated situations (i.e., the *Inv* mutant). To see how this might come about, we have to comprehend how a morphogen would be transported and mixed by the nodal flow. Mixing in the creeping flow in the node is very different to that we are more accustomed to seeing at higher Reynolds numbers, for example when we stir milk into our tea or coffee. In particular, turbulent mixing plays no role here; for there is no turbulence at low Reynolds numbers. We emphasize this as some articles on nodal flow have described the slow vortical flow in the *Inv* mouse as turbulent; it is not. What is seen in the node is always laminar flow, and the complex particle paths observed in low-Reynolds-number flows arise not from turbulence, but from another phenomenon, that of chaotic advection (Ottino, 1989; Cartwright et al., 1999).

We can understand some important aspects of mixing in creeping flows without explicitly solving the ARD equation by quantifying all the relevant processes beforehand. Advection can be quantified by an advective mixing time $\tau_a = L/U$, diffusion can be estimated by a diffusive mixing time $\tau_d = L^2/D_c$, and degradation or inactivation by a inactivation mean $\tau_i = 1/\kappa$ or half $\tau_{1/2} = \ln(2)/\kappa$ lifetime. With these three time scales, we can define two relevant dimensionless numbers: the Péclet number and the Damköhler number. The Péclet number measures the relative importance of advection and diffusion by the ratio $Pe = \tau_d/\tau_a = UL/D_c$ and it turns to be a highly conserved quantity among vertebrates. The product $U \cdot L$ falls in the range $1.5–2 \times 10^{-10}$ $m^2 s^{-1}$ for mouse, medakafish, and rabbit (Okada et al., 2005) given an estimated time $1 < \tau_a < 5$ s for a morphogen to be advected across the node in wild-type organisms. The Damköhler number, on the other hand, measures how the chemical reaction or degradation rate compares with the rate of diffusive transport $Da = \tau_d/\tau_i = \kappa L^2/D_c$. A good estimate for this number is lacking from current experimental results given the unknown nature of the transported morphogens. Finally, the product of these two dimensionless quantities $Pe \cdot Da = \tau_a/\tau_i = \kappa L/U$ compares the reaction rate and the advective transport time.

Molecular diffusion is independent of fluid flow and takes place at a rate determined by the diffusivity of the morphogen c, which depends on its molecular mass. For biological macromolecules like proteins, the diffusion coefficient D_c is typically in the range from 10^{-11} to 10^{-10} m^2 s^{-1}. We can then estimate a diffusive mixing time for a morphogen in the node, which lies in the range $25 < \tau_d < 250$ s. Hence, the Péclet number is in the range $5 < Pe < 250$; greater than unity—if it were not advection would be unimportant—but relatively small, so the con-

tribution of diffusion is fundamental to mixing and cannot be ignored.

The steady state solution of the ARD equation would then depend on the specific values of the relevant parameters, and one can envision three possible scenarios, all of which have been experimentally observed with the use of caged fluorescently labeled proteins (Okada et al., 2005):

(a) $\tau_i > \tau_d > \tau_a$ or

(b) $\tau_d > \tau_i > \tau_a$; in both cases, although the Péclet number is large, morphogen degradation is slow compared with the time necessary for diffusion, or, respectively, for advection. Therefore, the steady state solution is a uniform distribution of the morphogen.

(c) $\tau_d > \tau_a > \tau_i$; only if degradation is fast enough, will an asymmetric steady state distribution will be reached.

The important implication of this analysis for the biology is that the morphogen must be degraded and become inactive sufficiently rapidly after its release otherwise it would reach a constant concentration throughout the node and be of no use for initiating symmetry breaking through concentration differences.

With the constraints to the physical parameters given by this analysis, we can explicitly solve the ARD equation. However, to proceed, we need to define the appropriate initial and boundary conditions. There are a priori many possibilities for the positions of the sources and receptors of morphogen within the node. A series of models has been analyzed for compatibility with the genetic and biochemical evidence (Okada et al., 1999; Vogan and Tabin, 1999). We should, in addition, ask that the model be faithful to the fluid-dynamical, transport, and mixing properties of the nodal flow.

A model that fulfils these requirements was first developed by Cartwright et al. (2004) and later experimentally confirmed by Okada et al. (2005): A left–right asymmetric steady-state concentration profile was observed under left–right symmetric initial and boundary conditions.

In Figure 5, we exhibit the results of numerical simulations of this model in a rectangular domain representing the flow in a cross section of the node. In this case, we assume the morphogen to be released from the perinodal regions at the left and right edges of the node, and detected by receptors across the whole floor of the node. As the sources are in the upper part of the node, the morphogen finds itself to begin with in the upper recirculatory vortex. The morphogen coming from the right side is swept leftward across the node in the central leftward current, while that from the left side is pushed rightward across the roof of the node by the upper recirculatory vortex. While it is advected by the flow, the morphogen diffuses. Diffusion allows it to cross flow streamlines and so to come into contact with the receptors on the floor of the node. In a wild-type embryo the morphogen in the leftward current is swept to the left side of the node before it arrives by diffusion at the node floor and degrades. As a result, the steady-state active morphogen concentration pattern at the floor of the node is as shown in Figure 5c, with the maximum on the left. The analysis by Okada et al., although performed for slightly different initial and boundary conditions, confirms the behaviour predicted by the inspection of the ARD equation and its associated Péclet and Damköhler numbers.

However, there is still a missing ingredient in the previous analysis. Even though we took into account diffusive transport by means of a diffusion time τ_d, we have only considered so far horizontal diffusion in the node, neglecting any effect vertical diffusion may play in setting the steady-state concentration profile. If we quantify vertical diffusive time by $\tau^{vert}{}_d = d^2/D_c$, where d is the depth of the node, once we fix the Pe and Da numbers as before, we can recognize the existence of two possible scenarios: $\tau_d > \tau^{vert}{}_d > \tau_a$ or $\tau_d > \tau_a > \tau^{vert}{}_d$.

The characteristic vertical diffusion time to diffuse from the leftward flow a few microns above the floor of the node down to the floor is of order 0.25–2.5 s. If we compare this with the advection time across the node, 1–5 s for wild-type organisms, and twice as long or more for *Inv* mice, it is clear that on which side of the node the maximum concentration of morphogen reaches the node floor will depend crucially on this advection time. While for wild-type embryos the first scenario holds, with the slower nodal flow in *Inv* mice the advection time is longer and the second scenario is plausible. In that case, the diffusing morphogen arrives at the node floor on the right side of the node, and activates the right side receptors instead of the left. Shortly thereafter, the morphogen must become degraded, so that although it will continue circulating within the node, it is now in an inactive form and unable to dock with the receptors. As a result, the steady-state active morphogen concentration pattern at the floor of the node is reversed as shown in Figure 5d. This model thus explains the symmetry breaking seen in both wild-type and *Inv* mice. In the earlier delayed-activation model proposed by Okada et al. (1999), a signaling molecule is released at the left and right sides of the node in an inactive form, while receptors are present across the whole of the floor of the node. Some time after release, the molecule becomes activated and can dock with the receptors. Following this hypothesis, in a wild-type animal the activated morphogen would dock with more receptors on the left side, while in an *Inv* mouse the slower flow would allow the morphogen to become activated while still on the right side of the node, producing *situs inversus*. By taking into account the fluid dynamics we have seen that delayed activation is not necessary, although it is perfectly compatible with the model, as the molecular diffusion time from the central nodal current to the floor ensures that a morphogen does not immediately come into contact with its receptors. Furthermore, by taking into consideration the closed nature of the node and the recirculation pattern of flow it suggests, we see that while an activation time for the morphogen is not necessary, an inactivation time is. The morphogen must have a window of activity, between an initial time which could be zero (instant activation), or nonzero (delayed activation), and a final time less than τ_d, the diffusive mixing time in the node.

The plausibility of the above morphogen concentration model has by now been experimentally confirmed. Concentration gradients can indeed be generated by the appropriate balance of advection, diffusion and degradation. Although the aforemen-

tioned experiments were carried out only on wild-type embryos, these results combined with the observation that normal lateralization of *Inv* mutants can be rescued by an exogenous fast leftward flow (Watanabe et al., 2003), point to this balance of terms as being responsible for left–right determination.

The compatibility between the morphogen model and the available observations of course does not necessarily disprove the mechanosensing idea. The second population of monocilia observed in the node (McGrath et al., 2003) has been speculated to be mechanoreceptors for the flow. Moreover, it is known that monocilia possess the necessary biochemical machinery for both chemo- and mechanoreception (Pazour and Witman, 2003). However, the idea of the mechanical sensing of the shear stress on the node walls, or the velocities of the flow at the side walls, rather than a morphogen, being responsible for the symmetry breaking is improbable, the reason being the physics at hand. At low Reynolds number in Stokes flow the magnitudes of the shear stresses and flow velocities are symmetric across the node, leaving only their direction to break the symmetry. Mechanosensing of the flow by cilia (Pazour and Witman, 2003; Tabin and Vogan, 2003) could then provide the signal for symmetry breaking only if the sensors could detect not just the magnitude, but also the direction of the flow. Such a vectorial signal is produced, for example, by the hair cells of the ear (Roberts et al., 1988), but these are cells possessing bundles of cilia. For a monocilium to function thus, it would have to be long and flexible enough to sample different flow regimes when the flow was in one direction or the other; given the structure of the nodal flow, this seems unlikely. In the next section, however, we will see that the mechanosensing proposal may yet be reconciled with the facts.

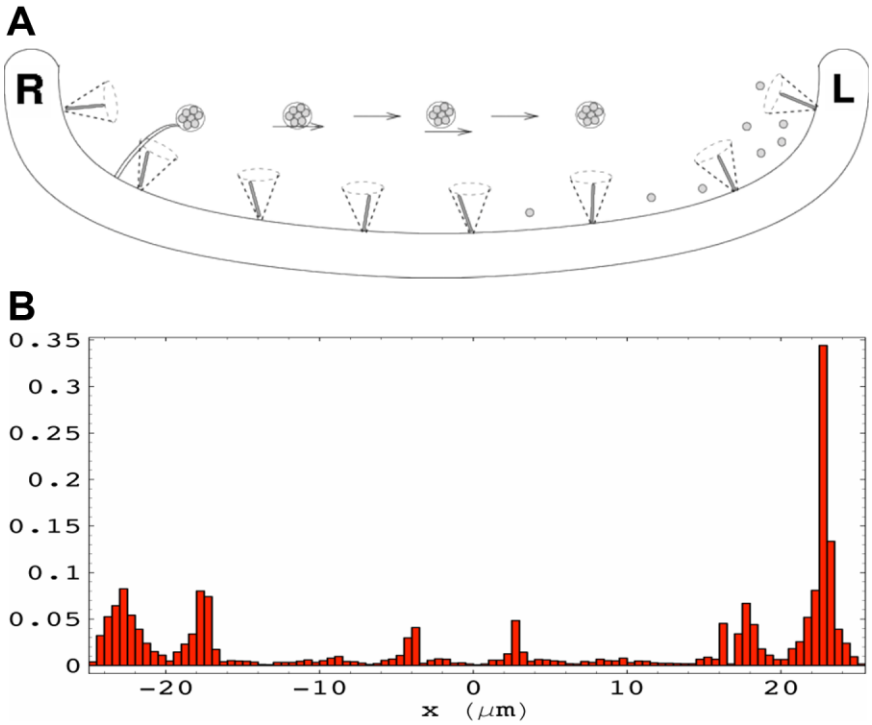

Fig. 6. **a:** Sketch of a vertical slice across the node viewed from the ventral side showing the monocilia producing the leftward flow that transports nodal vesicular parcels. **b:** Histogram showing the relative frequency with which a nodal vesicular parcel breaks as a function of its position from right to left along the floor of the node.

NODAL VESICULAR PARCELS

Even though the foregoing proposal was built on the assumption that morphogens are secreted molecule by molecule, which would suggest that the diffusion rate to be considered is molecular diffusion, the model still holds with the recently discovered fact that the morphogen is released in a discrete manner, in packets wrapped in a lipid vesicle known as nodal vesicular parcels (NVPs; Tanaka et al., 2005). These are natural passive tracers some 0.3–5 μm in diameter that contain morphogens (Sonic hedgehog and retinoic acid) within a lipid membrane. They are launched from microvilli and pass intact through the fluid flow, but break in proximity with the cilia and the walls of the node, to deliver there the morphogens they contain.

The NVPs are advected by the flow in the same way as individual morphogen molecules would be, but molecular diffusion has little effect on them. However, an effective diffusion rate stems from the disordered nature of the flow in the node, induced by so-called chaotic advection (Ottino, 1989; Cartwright et al., 1999). On the other hand, the role of the deactivation reaction can be now played by an effective life-time of the parcels. While this model is theoretically plausible, its validation or dismissal requires a new generation of experiments designed to investigate the fine details of the behavior of NVPs. One can think, for example of isolating NVPs to investigate their stability in controlled conditions.

The trajectories of the nodal vesicular parcels may be computed supposing them to be perfect passive tracers released at random points above the floor of the node. This simulates their experimentally observed origin as vesicles projected into the flow by microvilli, and released every 5–15 s (Tanaka et al., 2005). Again following the experimental observations, we may suppose their breakage when they collide with a wall or with a cilium. We can then collect the statistics corresponding to some hours of nodal flow of the position within the node at the moment of rupture of a large number of nodal vesicular parcels; we show the results of such a numerical experiment in the histogram of Figure 6. The outcome is similar for the in vivo and in vitro cases. Most of the nodal vesicular parcels are transported leftward across the node and collide with the left wall or with the

cilia nearest to it. The smaller intermediate peaks in the histograms indicate that a few are broken in other locations across the floor of the node by interactions with cilia there. This results suggest that no matter where the nodal vesicular parcels are released by the microvilli, and in particular if they are released in a symmetric manner across the node, they will most probably break near the left wall and deliver there their cargo of morphogen.

The foregoing idealizes the nodal vesicular parcels as passive tracers that follow faithfully the flow. The unknown here is the density of the nodal vesicular parcels; in the absence of further data, it is supposed that they are neutrally buoyant. The nodal vesicular parcels will most probably be close to neutrally buoyant: otherwise, if they were too light or too heavy, they would be propelled by centripetal or centrifugal forces to the middle or to the edges of the vortices in the node, which would make them of little use for their job of transporting materials across the node. Neutrally buoyant particles will faithfully follow a fluid flow as long as certain conditions on the flow apply: it should not deform fluid parcels to too great an extent; contrariwise particles will cease to follow pathlines of the flow (Babiano et al., 2000). These conditions on what in dynamical terms is the hyperbolicity of the flow probably break down precisely where the nodal vesicular parcels rupture.

A membrane will rupture if it is forced to stretch—to increase its surface area—beyond a critical threshold. Rupture generally occurs in biological membranes for a critical applied stress, the lysis tension, at which the membrane surface area has been increased by some 2–5% (Boal, 2002). To visualize how this applies here one may imagine the nodal vesicular parcels containing their cargo of morphogens as bags such as sacks of potatoes or beanbags. The bag, the membrane, is easily deformable without an increase in surface area if the bag is loosely filled, but if on the other hand it is completely filled, any attempt at deforming it leads to an increase in surface area, with the consequent possibility of breaking the bag, i.e., rupturing the membrane (as many people have discovered upon sitting on an overfilled beanbag). We should then consider two alternatives for the nodal vesicular parcels: either the membrane is taut, so that the vesicle is maintained approximately spherical, or it is slack, so the vesicle can deform from sphericity without breaking.

Images of nodal vesicular parcels attached to microvilli in the node show these projecting out from the nodal surface into the flow with an appending nodal vesicular parcel (Tanaka et al., 2005). This presumably adheres to its microvillus by electrostatic, van der Waals, or hydration forces. The microvillus could either actively release its nodal vesicular parcel by decreasing the adhesive forces, or else detachment could occur with no input on the part of the microvillus if the nodal vesicular parcel breaks away once the microvillus projects far enough out into the flow that the Stokes drag given by the local flow velocity exceeds the adhesive forces. It then circulates in the flow until it ruptures, apparently upon impact with a cilium or with the node wall, releasing its cargo of morphogens held within the membrane. Certainly NVPs appear to break in the vicinity of cilia or of the wall, but it is really an impact process? This would be remarkable, as this would suggest that any impact force should be much larger than the Stokes drag, something unlikely at the low Reynold number of the nodal flow. The average Stokes drag force suffered by the nodal vesicular parcels at the point of being released into the flow, taking them to be spherical, is given by $F_D=6\pi\mu Ur$. To obtain a conservative estimate, let us assume that the viscosity of the extraembryonic fluid is not dissimilar to that of water, $\mu\sim1$ mPa s, the average vesicle radius is $r\sim1$ μm, and the average node flow velocity is $U\sim4$ μm s^{-1}. This gives a force on the membrane at the moment of vesicle release of $F_D\sim8\times10^{-14}$ N, which is a lower bound, as some of the above terms could be an order of magnitude larger. On the other hand, the impact force suffered by the nodal vesicular parcels when they collide with a cilium or a wall can be estimated by Newton's second law as $F_I=m\Delta V/\Delta t=2/3\ \pi r^2\rho\Delta V^2/\beta$, where ρ is the density of the nodal vesicular parcel (which we shall assume to be similar to that of the extraembryonic fluid $\sim10^3$ kg m^{-3}), β is the fraction of its radius that the nodal vesicular parcel deforms during the collision and measures the packing within the nodal vesicular parcel; a loosely filled parcel can deform a great deal, while one tightly packed can deform only a tiny amount. If we consider that in the most energetic impact possible, a head-on collision with a cilium moving in the opposite direction, $\Delta V\sim100$ μm s^{-1}, we obtain $F_I\sim2\times10^{-19}/\beta$ N. This impact force is an upper bound on the force experienced by the membrane on impact: all the impact force would be transmitted to the membrane only if there were no internal dissipation of the impact energy, and consideration of the beanbag model of an NVP indicates that it is likely that much of the energy would be dissipated internally.

Because the vesicle ruptures during impact, and not during release, we suppose $F_I>F_D$, which would suggest $\beta<2.5\times10^{-6}$, that is to say the vesicle must be so tightly filled that it can only deform by at most a few parts per million before stretching its covering membrane to breaking point. If the membrane were this taut, it would certainly have ruptured previously; either the Stokes drag force experienced on release, or the deformation caused by shear within the viscous flow, would certainly rupture such a fragile structure within the flow long before it could deliver its cargo.

The inexorable conclusion of the physics is then that rather than just the mechanical breakage of the vesicles, there must exist an active rupture mechanism that acts upon the impact of the vesicle with a particular region of the node or the cilia (Cartwright et al., 2007). In other words, the vesicles are not broken by mechanical forces, so we must entertain the idea that contact of the vesicular membrane with something on the wall of the node or with certain cilia must destabilize the membrane by means presumably chemical in nature. The reported apparent swelling of the vesicles before rupture (Hirokawa et al., 2006) might well be a signature of this chemical destabilization. The swelling might be triggered by an opening of membrane channels on its surface or from osmotic pressure of the morpho-

gens inside the vesicle. Moreover, mutant mouse embryos in which nodal vesicular parcels are released, but cilia are immobile, offer a datum in favor of this argument that there is an undiscovered biochemical rupture process for the nodal vesicular parcels. In these embryos, rupture of nodal vesicular parcels appears to occur even without flow (Tanaka et al., 2005). If in this mutant the flow mechanism is faulty, but the—separate—biochemical contact rupture mechanism is functioning, these results are explained. Might the active regions involved in this rupture mechanism be associated with the second population of apparently immotile cilia found toward the sides of the node (McGrath et al., 2003)? This idea would serendipitously unite the rival morphogen and two-cilia models of how nodal flow is interpreted by the embryo: these cilia could be mechanosensors as originally postulated in the two-cilia model, while concurrently acting to break up the nodal vesicular parcels by means of a biochemical mechanism to release the morphogens within as hypothesized in the earlier morphogen model. But the chemical signal would not have to be localized to the periphery of the node for the nodal vesicular parcels to dissociate primarily in this location; that remains a function of the frequency with which they arrive in proximity with the wall at different locations across the node. We look forward to the experimental investigation of this proposal and to more research into NVPs in general.

SHORT PERSPECTIVES

Symmetry breaking is at the heart of modern developments in the physical sciences. Physicists from the second half of past century onward have developed a great repertoire of methods to explain a wide range of phenomena in terms of this process. Biological symmetry breaking in particular has also long interested physical scientists. In 1952, Turing pioneered the explanation of morphogenesis and its (bio)chemical basis in terms of a mechanism of pattern formation induced by the interaction of diffusing morphogens that now bears his name (Turing, 1952). However, even at that early stage, he recognized the special problem for his theory posed by left–right symmetry breaking in vertebrates: nature almost always breaks left–right symmetry in a given sense, whereas his mechanism would lead to approximately equal numbers of animals with *situs inversus* and *situs solitus*. His proposed solution to this puzzle was that the inputs to the system must somehow be biased. Almirantis and Nicolis (1987) built on this idea and showed in detail how an initial gradient could seed the process. Later, Brown and Wolpert (1990) introduced the hypothesis of a chiral molecule with a fixed orientation relative to the anterior–posterior and dorsal–ventral axes, as a messenger of the necessary information regarding left and right to produce the initial bias. But it seems that nature, in mice at least, prefers to use not a chiral molecule, but another chiral structure—a molecular motor—to elicit advective transport in a well-defined direction relative to the anterior–posterior and dorsal–ventral axes and thence to trigger lateralization. The information on which side is which is then carried to the rest of the embryo by diffusion. Hamada et al. (2002) proposed that the subsequent phase of propagation of the broken symmetry could even function by exactly the mechanism Turing imagined, with the initial small concentration difference produced by the nodal flow magnified by a nonlinear interaction between two diffusing proteins, Nodal and Lefty. A further possibility is that the interaction may involve the fluid flow itself, which would make this a biological instance of a generalized Turing pattern-formation mechanism including fluid flow (Satnoianu et al., 2001).

While diffusion is ubiquitous in biology, nature also often uses advection to achieve its ends, for example in the cardiovascular system, and it has recently been found to be fundamental in the development of the heart (Hove et al., 2003). The use of cilia to move fluid is also common, for example in the lung. Microbes use cilia and flagella for propulsion, just as the node uses them to advect fluid, and the similarity of scale suggests a similarity of environment. This highlights the resemblance of the situation in the node to that of microbial swimming. In both cases, we are talking of life at low Reynolds number (Purcell, 1977). The problems of moving fluids at the microscale, with their associated low Reynolds numbers, are also now interesting engineers who design fluid flow microsystems; so-called microfluidics devices (Gad-el-Hak, 1999). We humans inhabit a world of much higher Reynolds number, and our intuition on how fluids behave is not straightforwardly transferable into this alien inertialess environment, which is why some ideas put forward for producing a directional flow from rotating cilia cannot work, because there is no fluid inertia. Producing the nodal flow is not like waving your arms about in a swimming pool (Whitfield, 2002), but more akin to finding oneself "in a swimming pool that is full of molasses, and . . . forbid(den) . . . to move any part of (the) body faster than 1 cm/min" (Purcell, 1977). While differences in the cilium stroke during different parts of the rotation cycle have, it seems, been observed (Okada et al., 2005), it is a conceptual mistake to assign functionality to this phenomenon, at least in terms of the generation of the flow at these scales. Rather, we are inclined to believe that such nonuniform motion is the emergent consequence of the cilium being a complex but symmetric slender elastic body rotating around a tilted axis and very close to a wall. In the nodal environment, nine orders of magnitude lower in Reynolds number than the above person in a swimming pool, the lack of inertia constrains the fluid physics that the biology can exploit, leaving the proposed mechanisms of a posterior tilt of the cilia and the chemosensing of the flow as the best fundamental hypotheses, compatible with the facts, for producing the observations reported in experiments. A proper understanding of the effects of boundary conditions is, of course, necessary only for the detailed description of other less fundamental processes.

While the work reviewed here addresses experiments on mice, it has been surmised that the mechanism possesses a great deal of universality among vertebrates. In fact, similar

structures to the node with its monocilia are found in other vertebrate embryos (Essner et al., 2002). On the other hand, there is other experimental evidence showing asymmetries in chick and frog embryos before the emergence of the nodal structures (Mercola, 2003). If these observations are correct, then nodal flow is not the earliest left–right symmetry breaking event in some vertebrates. If the initial symmetry-breaking mechanism differs across species, the chiral molecule or structure, equivalent to the chiral monocilium of the node, that bootstraps the process must be sought for those cases. Moreover, the role of the nodal flow in those species would need to be clarified: would it then be acting as a means to preserve or amplify an initial asymmetric signal from the earlier symmetry-breaking event, or would it constitute a second, independent, mechanism for determining left and right? Might this be a case of two independent mechanisms creating extra robustness through redundancy? More evidence needs to be collected. However, independently of whatever turn out to be the right answers to these questions, the established facts about the nodal flow teach us again a necessary, but often forgotten, lesson that genetic programs can make use of far more physical laws and processes than merely those acting at a molecular level. This is a rather clear instance, for example, where genetics has taken into account the macroscopic laws of fluid mechanics, including, perhaps rather subtle phenomena involving advection and diffusion.

ACKNOWLEDGMENTS

J.H.E.C. was funded by the Spanish Ministerio de Ciencia y Tecnología, O.P. was funded by the Intramural project of the CSIC agency HIELOCRIS, and I.T. was funded by the Human Frontier Science Program.

REFERENCES

Almirantis Y, Nicolis G. 1987. Morphogenesis in an asymmetric medium. Bull Math Biol 49:519–530.

Babiano A, Cartwright JHE, Piro O, Provenzale A. 2000. Dynamics of a small neutrally buoyant sphere in a fluid and targeting in Hamiltonian systems. Phys Rev Lett 84:5764–5767.

Batchelor GK. 1970. The stress system in a suspension of force-free particles. J Fluid Mech 41:545–570.

Blake JR. 1972. A model for the microstructure in ciliated organisms. J Fluid Mech 55:1–23.

Blake JR, Otto SR. 1998. Filter feeding, chaotic filtration, and a blinking Stokeslet. Theor Comput Fluid Dyn 10:23–36.

Boal D. 2002. Mechanics of the cell. New York: Cambridge University Press.

Brennen C, Winet H. 1977. Fluid mechanics of propulsion by cilia and flagella. Annu Rev Fluid Mech 9:339–398.

Brokaw CJ. 1972. Flagellar movement - a sliding filament model - an explanation is suggested for spontaneous propagation of bending waves by flagella. Science 178:455–462.

Brokaw CJ. 2005. Computer simulation of flagellar movement IX. Oscillation and symmetry breaking in a model for short flagella and nodal cilia. Cell Motil Cytoskeleton 60:35–47.

Brown NA, Wolpert L. 1990. The development of handedness in left/right asymmetry. Development 109:1–9.

Buceta J, Ibañes M, Rasskin-Gutman D, Okada Y, Hirokawa N, Izpisúa-Belmonte JC. 2005. Nodal cilia dynamics and the specification of the left/right axis in early vertebrate embryo development. Biophys J 89:2199–2209.

Cartwright JHE, Feingold M, Piro O. 1999. An introduction to chaotic advection In: Chaté H, Villermaux E, Chomez JM, editors. Mixing: chaos and turbulence. Amsterdam: Kluwer. p 307–342.

Cartwright JHE, Magnasco MO, Piro O. 2002. Noise- and inertia-induced inhomogeneity in the distribution of small particles in fluid flows. Chaos 12:489–495.

Cartwright JHE, Piro O, Tuval I. 2004. Fluid-dynamical basis of the embryonic development of left-right asymmetry in vertebrates. Proc Natl Acad Sci U S A 101:7234–7239.

Cartwright JHE, Piro N, Piro O, Tuval I. 2007. Embryonic nodal flow and the dynamics of nodal vesicular parcels. J R Soc Interface 4:49–56.

Chwang AT, Wu TYT. 1975. Hydromechanics of low-Reynolds-number flow. Part 2. Singularity method for stokes flows. J Fluid Mech 67:787–815.

Currie IG. 1993. Fundamental mechanics of fluids. New York: McGraw Hill.

Dillon RH, Fauci LJ. 2000. An integrative model of internal axoneme mechanics and external fluid dynamics in ciliary beating. J Theor Biol 207:415–430.

Essner JJ, Amack JD, Nyholm MK, Harris EB, Yost J. 2005. Kupffer's vesicle is a ciliated organ of asymmetry in the zebrafish embryo that initiates left-right development of the brain, heart, and gut. Development 132:1247–1260.

Essner JJ, Vogan KJ, Wagner MK, Tabin CJ, Yost HJ, Brueckner M. 2002. Left-right development: conserved function for embryonic nodal cilia. Nature 418: 37–38.

Gad-el-Hak M. 1999. The fluid mechanics of microdevices. J Fluids Eng 121:5–33.

Gueron S, Liron N. 1992. Ciliary motion modeling, and dynamic multicilia interactions. Biophys J 63:1045–1058.

Gueron S, Levit-Gurevich K, Liron N, Blum JJ. 1997.Cilia internal mechanism and metachronal coordination as the result of hydrodynamical coupling. Proc Natl Acad Sci U S A 94:6001–6006.

Hamada H, Meno C, Watanabe D, Saijoh Y. 2002. Establishment of vertebrate left-right asymmetry. Nat Rev Genet 3:103–113.

Hancock GJ. 1953. The self-propulsion of microscopic organisms through liquids. Proc R Soc Lond A 217:96–121.

Hirokawa N, Tanaka Y, Okada Y, Takeda S. 2006. Nodal flow and the generation of left-right asymmetry. Cell 125:33–45.

Hove JR, Köster RW, Forouhar AS, Acevedo-Bolton G, Fraser SE, Gharib M. 2003. Intracardiac fluid forces are an essential epigenetic factor for embryonic cardiogenesis. Nature 421:172–177.

Kramer-Zucker AG, Olale F, Haycraft CJ, Yoder BK, Schier AF, Drummond IA. 2005. Cilia-driven fluid flow in the zebrafish pronephros, brain and Kupffer's vesicle is required for normal organogenesis. Development 132:1907–1921.

Lighthill MJ. 1976. Flagellar hydrodynamics. The Jon von Neumann lecture. SIAM Rev 18:161–230.

McGrath J, Somlo S, Makova S, Tian X, Brueckner M. 2003. Two populations of node monocilia initiate left-right asymmetry in the mouse. Cell 114:61–73.

Meleshko VV, Aref H. 1996. A blinking rotlet model for chaotic advection. Phys Fluids 8:3215–3217.

Mercola M. 2003. Left-right asymmetry: nodal points. J Cell Sci 116:3251–3257.

Nonaka S, Tanaka Y, Okada Y, Takeda S, Harada A, Kanai Y, Kido M, Hirokawa N. 1998. Randomization of left-right asymmetry due to loss of nodal cilia generating leftward flow of extraembryonic fluid in mice lacking KIF3B motor protein. Cell 95:829–837.

Nonaka S, Shiratori H, Saijoh Y, Hirokawa N. 2002. Determination of left-right patterning of the mouse embryo by artificial nodal flow. Nature 418:96–99.

Nonaka S, Yoshiba S, Watanabe D, Ikeuchi S, Goto T, Marshall WF, Hamada H. 2005. De novo formation of left-right asymmetry by posterior tilt of nodal cilia. Plos Biol 3:e268.

Okada Y, Nonaka S, Tanaka Y, Saijoh Y, Hamada H, Hirokawa N. 1999. Abnormal nodal flow precedes situs inversus in iv and inv mice. Mol Cell 4:459–468.

Okada Y, Takeda S, Tanaka Y, Izpisúa-Belmonte JC, Hirokawa H. 2005. Mechanism of nodal flow: a conserved symme-

try breaking event in left-right axis determination. Cell 121:633–644.
Ottino JM. 1989.The kinematics of mixing: stretching, chaos, and transport. New York: Cambridge University Press.
Pazour GJ, Witman GB. 2003. The vertebrate primary cilium is a sensory organelle. Curr Opin Cell Biol 15:105–110.
Purcell EM. 1977. Life at low Reynolds number. Am J Phys 45:3–11.
Roberts WM, Howard J, Hudspeth AJ. 1988. Hair cells: transduction, tuning, and transmission in the inner ear. Annu Rev Cell Biol 4:63–92.
Satnoianu RA, Maini PK, Menzinger M. 2001. Parameter space analysis, pattern sensitivity and model comparison for Turing and stationary flow-distributed waves (FDS). Physica D 160:79–102.
Smith DJ, Gaffney EA, Blake JR. 2007. Discrete cilia modelling with singularity distributions: application to the embryonic node and the airway surface liquid. Bull Math Biol 69:1477–1510.
Smith DJ, Blake JR, Gaffney EA. 2008. Fluid mechanics of nodal flow due to embryonic primary cilia. J R Soc Interface 5:567–573.
Tabin CJ, Vogan KJ. 2003. A two-cilia model for vertebrate left-right axis specification. Genes Dev 17:1–6.
Tanaka Y, Okada Y, Hirokawa N. 2005. FGF-induced vesicular release of Sonic hedgehog and retinoic acid in leftward nodal flow is critical for left-right determination. Nature 435:172–177.
Turing AM. 1952. The chemical basis of morphogenesis. Philos Trans R Soc Lond B 237:37–72.
Vogan KJ,Tabin CJ. 1999. Developmental biology: a new spin on handed asymmetry. Nature 397:295–298.
Watanabe D, Saijoh Y, Nonaka S, Sasaki G, Ikawa Y, Yokoyama T, Hamada H. 2003. The left-right determinant Inversin is a component of node monocilia and other 9+0 cilia. Development 130: 1725–1734.
Whitfield J. 2002. Embryos grow with the flow. Nat Sci Update 4 July.